Spectroscopic study of molecular-hydrogen processes in a mirror-confined plasma

Thomas G. Moran
Applied Research Corp., 8201 Corporate Drive, Landover, Maryland 20783
and NASA Goddard Space Flight Center, Code 693, Greenbelt, Maryland 20770
(Received 22 November 1993)

Visible and near-ultraviolet molecular hydrogen emission from the Tara Tandem Mirror central cell plasma was investigated in order to determine molecular densities, ionization rates, and continuum dissociation rates. Measurements of H_2 $G \rightarrow B$ band emission were used to infer spatial density and ionization profiles, maximum densities of 4×10^{12} cm^{-3} at the gas injection port, and a total molecular ionization rate of 254 A. Continuum emission in the near ultraviolet was identified as the H_2 dissociative continuum through its wavelength distribution, time behavior, and intensity. Wavelength-integrated continuum emission measurements were used to obtain the dissociation rate associated with the continuum: 6 A. The power expended in molecular ionization, dissociation, and radiation is estimated to be 8.4 kW out of 300 kW of rf power injected.

PACS number(s): 52.20.Fs, 33.20.Kf, 33.70.−w, 34.50.Gb

I. INTRODUCTION

Molecular ionization and dissociation processes play a key role in the fueling of hydrogen plasmas. Typically, molecular hydrogen gas is injected into magnetically confined hydrogen plasmas where it is dissociated or ionized through electron collisions, providing hydrogen atoms, protons, and electrons. These dissociation and ionization processes may be investigated through spatially resolved line and continuum emission measurements which, combined with measurements of electron temperature and density, yield molecular densities, and ionization and continuum dissociation rates. Line emission measurements can also be used to obtain the molecular dissociative-excitation contribution to atomic hydrogen line emission (e.g., H_α radiation), allowing atomic densities and ionization rates to be determined unambiguously from emission measurements. In addition, molecular emission measurements may be used to estimate the power expended in molecular dissociation, ionization, and radiation.

The Tara Tandem Mirror central cell [1,2] provided an excellent opportunity to investigate molecular hydrogen emission from a magnetically confined plasma. The vessel was designed for easy diagnostic access, with ports distributed at multiple locations along the device axis. Multiple-chord emission measurements across the plasma cross section were made at two axial locations. Measurements of edge chord emission were made possible by the close proximity of the ports to the plasma. Furthermore, plasma conditions in the Tara central cell were ideal for molecular spectral studies; molecules penetrated several centimeters into the plasma due to the low electron densities. In a higher density tokamak plasma, molecules would be located only in an outer cylindrical shell a few millimeters thick. In addition, electron temperatures in the Tara central cell edge plasma were typically 100 eV, making excitations to all bound energy states possible. Finally, impurity concentrations in the Tara central cell plasma were relatively low (0.6±0.2%) [3] and therefore impurity line contamination did not prevent molecular spectra measurements. Molecular emission measurements included line-resolved band emission in the visible and continuum emission in the near ultraviolet. Line intensities were used to obtain densities and ionization rates and the rate of continuum dissociation was estimated from the wavelength-integrated continuum emission.

This paper presents a brief description of the Tara confinement device and spectroscopic instrumentation in Sec. II. The data, analysis, and conclusions are presented in Secs. III, IV, and V, respectively.

II. EXPERIMENTAL APPARATUS

A. The Tara Tandem Mirror

A tandem mirror is a multiple magnetic mirror plasma confinement device designed to confine a cylindrical "central cell" plasma, both magnetically, using high field end coils, and electrostatically, using high electrical potentials created in mirror-confined end cell plasmas, or "plugs" [4–6]. The Tara Tandem Mirror central cell was comprised of cylindrical aluminum vacuum vessel 10 m long and 0.5 m in diameter, surrounded by magnetic field coils at 30 cm intervals. Titanium getters coated the inner vessel wall with titanium. Gas was injected through a port located in the "gas box," a 1 m baffled section located in the center of the central cell vacuum vessel. Baffles prevented gas from leaving the gas box without encountering the plasma. The magnetic field in the gas box was raised 10% above the average central cell field in order to create a magnetic "hill," which forced newly created plasma particles to stream out and fill the central cell. The discharge was initiated by injection of microwave radiation at the electron cyclotron frequency for initial ionization, followed by injection of radio frequency (rf) power at the ion cyclotron resonance frequency for plasma heating. Ions were heated directly by cy-

clotron resonance heating and electrons were heated through electron-ion collisions. Discharges were 60 ms long.

The Tara central cell was equipped with a varied set of diagnostic instruments which routinely measured plasma parameters and edge gas pressure. Electron density and temperature were measured using microwave interferometry and Thomson scattering, respectively, and ion temperature was measured with a charge-exchange atomic energy analyzer. Plasma pressure was inferred from diamagnetic loops measurements. Edge gas pressure was measured with fast-ion gauges (FIG's).

B. The spectrometer

Spectroscopic measurements were made with an ISA $f/4.7$, 0.6 m Czerny-Turner spectrometer equipped with a 10×10 cm^2, 2400 lines/mm diffraction grating, a Princeton Instruments optical multichannel analyzer (OMA), and a Hamamatsu R928 photomultiplier (PMT) housed in a magnetic shield. Light was directed to either the OMA or the PMT by a rotatable mirror located inside the spectrometer near the output port. The OMA consists of a linear 512 element light-intensified diode array with its own control electronics. The OMA was controlled by a VAX 11/780 computer through a Camac Crate interface system. Output from the photomultiplier was digitized at 5 kHz, then transferred to the VAX hard disk.

An absolute intensity calibration of the spectrometer in PMT mode from 2000 to 7000 Å was performed using an Optronics tungsten ribbon lamp which had been absolutely calibrated at NIST. The same lamp was used to perform a relative intensity calibration of the spectrometer in OMA mode from 4000 to 5000 Å, the region of interest for line spectra. Order-sorting filters were used to block second order light. The uncertainty in the lamp calibration was 10% and the shot noise was estimated at 1–4 % for a total uncertainty of 12%. Wavelength resolution was determined by recording mercury lamp line spectra at several wavelengths in the near-ultraviolet and visible range. The typical slit width of 20 μm yielded a resolution of 0.65 Å in OMA mode and 0.3 Å in PMT mode. The OMA mode resolution was degraded due to the light intensifier.

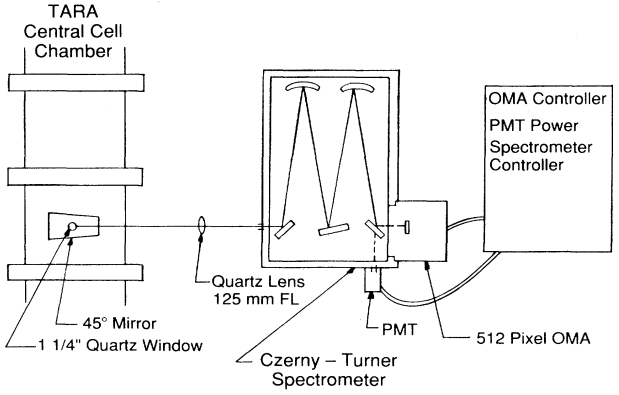

FIG. 1. Schematic diagram of the spectrometer mounted next to the Tara central cell at the gas injection port.

The spectrometer was moved among four axial locations along the central cell: two locations in the gas box (0 and 30 cm, with the injection port at 0 cm) and two to the north of the gas box (110 and 350 cm). At 0 and 30 cm light was collected through 3 cm diameter quartz windows mounted at the bottom of the vacuum vessel. Due to the small window diameter, emission measurements were limited to the central chord. At 110 and 350 cm light was collected using rotatable mirrors mounted close to a 10×30 cm^2 glass window (at 110 cm) and a 10 cm diameter quartz window (at 350 cm). A schematic diagram of the instrument mounted at a gas box location is shown in Fig. 1.

III. SPECTROSCOPIC MEASUREMENTS

A. Line spectra measurements

Molecular line and band emission from magnetically confined plasmas has been investigated previously at two experiments: the Alcator C tokamak [7,8] and the ELMO bumpy torus (EBT) device [9,10]. Terry [7,8] made single-chord measurements of ultraviolet Lyman band emission from the Alcator C tokamak plasma. Individual lines were not resolved, due to insufficient wavelength resolution, but characteristic band structures were identified. The measurements were used to obtain molecular and electron temperatures at the plasma edge by matching measured and synthetic spectra. McNeil [9,10] made single-chord measurements of line-resolved visible ($\sim$6000 Å) Fulcher band emission on the EBT device, identifying this band as the source of the high background emission measured in the EBT Thomson scattering experiment.

The molecular hydrogen lines chosen for the Tara spectra study belong to the $G\rightarrow B$ band and have wavelengths between 4000 and 5000 Å. This band results from decays of the singlet Rydberg state $G\,^1\Sigma_g^+(G)$ to the B state. The G state was originally classified as a distinct state by Dieke [11], but more recent work has shown that this state couples adiabatically with the doubly excited $K\,^1\Sigma_g^+(K)$ state, resulting in a combined state designated $GK\,^1\Sigma_g^+(GK)$ which has a double-minimum potential curve [12,13]. However, for spectroscopic purposes the G and K states can be considered distinct, since each state produces its own line spectrum. Plots of the X, GK, and B potential curves are shown in Fig. 2.

The $G\rightarrow B$ lines were chosen for this study because they contain the most intense lines for electron energies over 20 eV [14], their wavelengths lie near the peak of the OMA response curve, and the largest emission cross sections in the band have been measured for energies between 15 and 300 eV [15]. Fulcher band lines were present in the Tara spectrum, but their detected signals were a factor of 100 lower than those of the $G\rightarrow B$ band lines, due to their smaller excitation cross sections at the 100 eV Tara electron temperatures and to the weaker OMA response at 6000 Å. The measurements include "lines" (some "lines" are actually blends of two or three

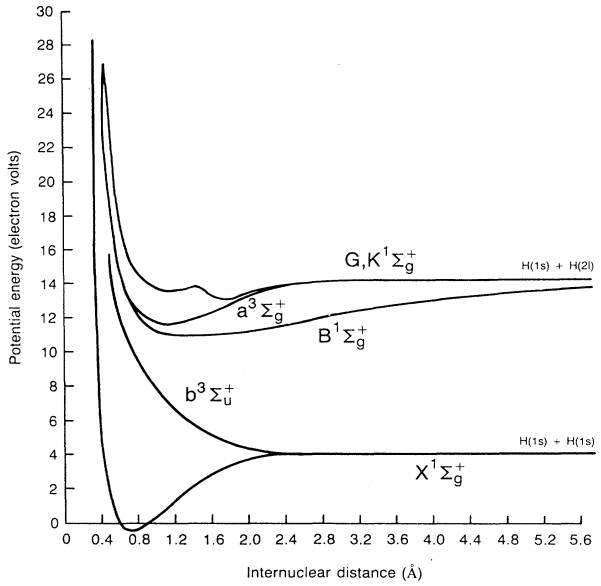

FIG. 2. Plot of the $X\ ^1\Sigma_g^+$, $GK\ ^1\Sigma_g^+$, $B\ ^1\Sigma_u^+$, $a\ ^3\Sigma_g^+$, and $b\ ^3\Sigma_u^+$ potential curves.

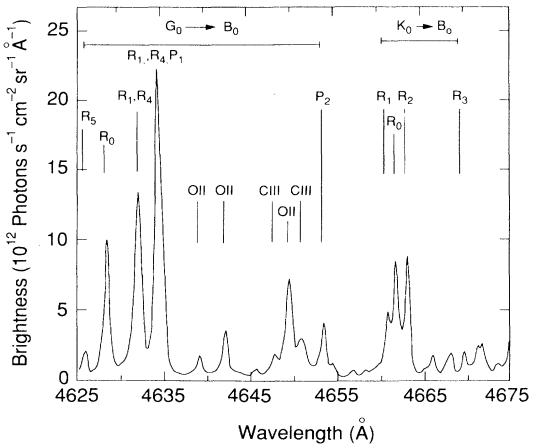

FIG. 3. Plot of the gas port spectrum between 4625 and 4675 Å measured along a central chord. Molecular lines are identified by band and rotational transition. Several impurity lines are also identified.

transitions) from several vibrational bands in the $G \rightarrow B$ system. The Tara study focused on two wavelength regions, 4180–4230 and 4625–4675 Å, which contain lines from the (0,1) and (0,0) bands, respectively.

Line emission measurements were made using the spectrometer in OMA mode at the 0, 30, and 110 cm locations. Emission levels at 350 cm were below the detection limit. Central chord atomic hydrogen H_α emission and electron density were monitored at several axial locations during the molecular spectra study to ensure plasma consistency. All measurements were repeated at least ten times and were easily reproduced. The OMA was gated on for 10 ms exposures, starting 10 ms after discharge initialization, and was exposed for 10 ms after the discharge ended in order to measure the background spectrum, which was subtracted from each plasma spectrum.

The strongest molecular line emission was measured at the gas injection port. Figure 3 shows a plot of the central chord gas port spectrum between 4625 and 4675 Å, with molecular lines labeled by vibrational band and rotational transition. Here G_n and K_n signify decays from the nth vibrational level of the G and K states, and P_m and R_m refer to decays from the mth rotational level, where the rotational quantum number j changes by $+1$ or -1, respectively. All of the labeled transitions go the $v=0$ vibrational level of the B state, B_0. Several CIII and OII lines in the spectrum are also labeled. There are five lines from the G_0 level and four lines from the K_0 level present. For comparison, a plot showing a H_2 spectrum in the 4625–4675 Å region made at 0.5 Å resolution is shown in Fig. 4, with the vibrational bands labeled. This spectrum was obtained by bombarding a beam of H_2 at 300 K with a beam of 100 eV electrons [16]. All of the lines in the beam spectrum are present in the Tara spectrum shown in Fig. 3, at approximately the same relative strengths. Measurements of the 4625–4675 spectrum made at 30 and 110 cm showed that the molecular intensities decreased dramatically with distance from the gas port, while impurity intensities showed a smaller drop. A plot of the gas port spectrum in the 4180–4230 Å range is shown in Fig. 5, with molecular and impurity lines labeled. The 4180–4230 Å molecular intensities also decreased with distance from the gas port, with the intensity ratio between the (0,0) and (0,1) bands remaining constant.

Figure 6 shows a plot of the central chord intensity of the 4634 Å line intensity as a function of distance from the gas port. The intensity decreases by a factor of 10 between 0 and 30 cm, and a factor of 4 between 30 and 110 cm. Also plotted for comparison are the central chord atomic hydrogen H_α brightness and FIG pressure. The

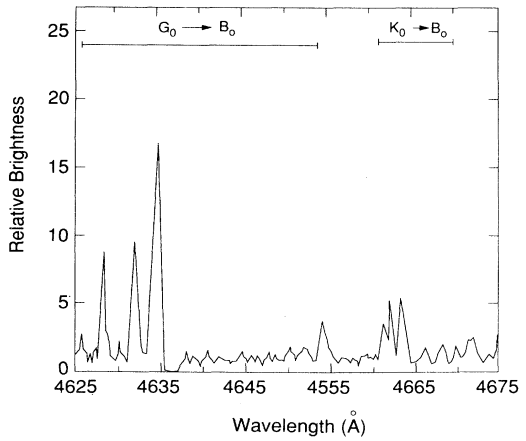

FIG. 4. Plot showing the H_2 spectrum between 4625 and 4675 Å emitted from a H_2 beam bombarded by 100 eV electrons [15].

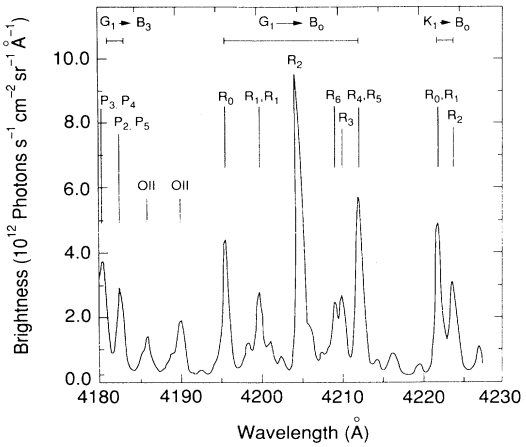

FIG. 5. Plot of the gas port spectrum between 4180 and 4230 Å measured along a central chord. Molecular lines are identified by band and rotational transition. Several impurity lines are also identified.

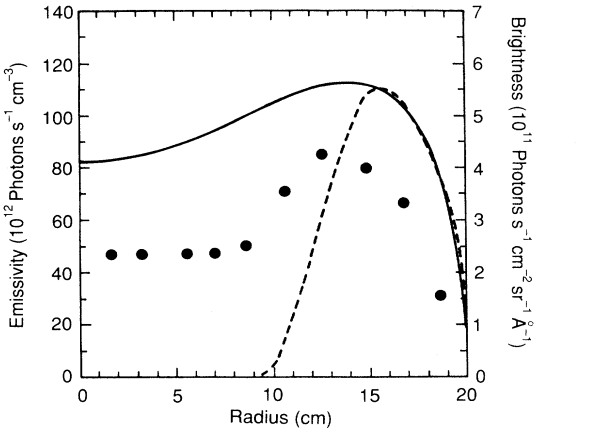

FIG. 7. Plot of the 4205 Å H_2 line brightness versus chordal radius at 110 cm (solid circles) and corresponding emissivity profile (dashed lines). Also plotted is the H_α emissivity profile at the same axial position [3] (solid line).

electron density was independent of z. Like the molecular emissivity, the atomic emissivity decreased with distance from the gas port, with the ratio between the emissivities remaining nearly constant over almost two orders of magnitude.

At 110 cm the radial brightness profile of the 4205 Å line was measured using the chordal scanning system and is shown in Fig. 7. The 4205 Å line was chosen for radial brightness measurements because of its relatively high intensity and isolation from impurity lines. The profile differs markedly from the atomic H_α radial profile, which was measured at the same location with the same instrument, and showed the atomic brightness peaked at the plasma center [3]. The radial emissivity profile E was computed from the measured brightness B by inverting Abel's integral equation and is plotted in Fig. 7. The inversion procedure produced a small negative emissivity inside a radius of 8 cm, which was an artifact of the inversion procedure, and the emissivity in this range was fixed at zero. The radial atomic hydrogen H_α emissivity profile from the same location is plotted along with the molecular profile for comparison. Note that the molecular emission is confined to an outer shell while the atomic emission penetrates to the center.

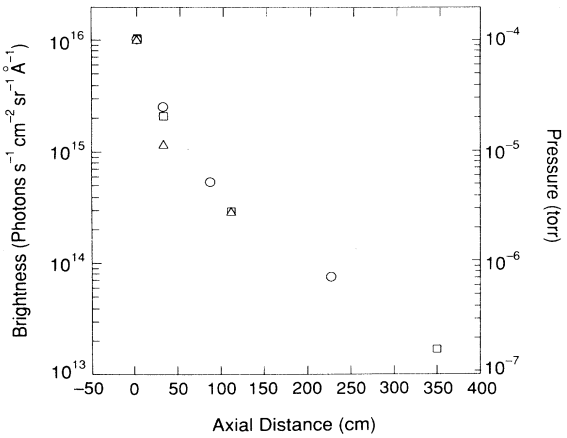

FIG. 6. Plots of the central chord 4634 Å H_2 line intensity multiplied by 500 (triangles), central chord H_α brightness (squares), and FIG pressure (circles) as a function of distance from the gas port.

B. Continuum spectra measurements

Electron bombardment of molecular hydrogen produces the well-known "dissociative continuum," which extends from the vacuum ultraviolet through the visible (1600–5000 Å) [17,18], and is utilized as a broadband uv light source in H_2 and D_2 lamps. The emission is produced through electron collisional excitation of H_2 in the singlet ground state X to the triplet excited states $a\ ^3\Sigma_g^+$:

$$e+H_2 \rightarrow H_2(a)\ , \tag{1}$$

where $H_2(a)$ denotes H_2 in the a state. This transition is spin forbidden and as a result the most probable transition following excitation to the a states is decay to the unbound triplet state $b\ ^3\Sigma_u^+$ followed by dissociation into two ground state atoms and photon emission:

$$H_2(a) \rightarrow H_2(b) \rightarrow H(1s)+H(1s)+h\nu\ , \tag{2}$$

where $H_2(b)$ denotes H_2 in the b state and $h\nu$ represents the emitted photon. Since the b state is unbound, there is a continuum of final molecular states, and therefore of photon energies. The potential energy curves of the X,a, and b states [19] are shown in Fig. 2.

Excitation of any vibrational level of a from any vibrational level of X is possible in principle. Decays from each vibrational level of a will produce a characteristic continuum spectrum. Continuum spectra from the $v'=0-15$ vibrational levels of a have been calculated

[20], and show that levels with $v' \geq 5$ emit almost entirely at wavelengths below 2000 Å, the lower wavelength limit of our measurements. Continua produced by levels with $v' < 5$ have brightness maxima between 2000 and 2400 Å, with emission from higher v' levels peaking at progressively lower wavelengths. The calculated continuum distribution for the $v'=0$ level has been verified by an experiment [21], but individual wavelength distribution measurements for higher v' levels have not been reported.

The dissociative continuum has been proposed as a source of plasma emission in two magnetic plasma confinement devices: the Deca II device [22] and the Alcator C tokamak [8]. Broadband emission from the Deca II hydrogen plasma between 2000 and 4000 Å was measured using wideband [700 Å full width at half maximum (FWHM)] optical filters. Continuum intensities were a factor of 1000 larger than what would have been expected from bremsstrahlung and recombination radiation, and the dissociative continuum was suggested as the cause. Measurements of H_2 Lyman band emission between 1200 and 1800 Å from the Alcator C gas injection port plasma showed the presence of a strong wavelength independent background emission at the gas port, which was identified as a combination of dissociative and Lyman continua. Neither the Deca II nor the Alcator C investigations found any intensity variations with wavelength in the continuum spectrum as predicted by theory, probably due to the large width of the optical filters in the case of the Deca II study and to the large overlapping band and Lyman continuum emission in the case of the Alcator C study.

The H_2 visible line spectra measurements demonstrated the presence of significant background emission at 0, 30, and 110 cm, which was proportional in intensity to the H_2 line emission, suggesting a molecular origin. Further measurements were made in the near ultraviolet where emission from the $v'=0$ level of the a state peaks using the spectrometer in PMT mode, since the OMA was not sensitive at those wavelengths. A plot of the gas port continuum brightness versus time is shown in Fig. 8, along with the axially integrated atomic hydrogen H_α emission and radially integrated electron density. Note that the continuum time behavior approximates the axially integrated H_α behavior, with an initial large "burnout spike" followed by nearly constant emission for the duration of the discharge. The two major differences are a steady rise in continuum emission during the discharge and a continuum spike at 60 ms, when the electron density begins to decline. The rise in continuum emission during the plasma might be due to changes in the gas box electron temperature or molecular density. The emission spike at 60 ms might be caused by either an increase in H_2 influx or an electron temperature drop, since the excitation rate increases strongly with decreasing electron temperature at 100 eV [23].

A wavelength intensity scan in the near ultraviolet from 2200 to 3600 Å at the gas port performed on a sequence of plasmas with nearly constant electron density and edge pressure (variations were less than 5%) is shown in Fig. 9. Brightness values shown were obtained by averaging over a 10 ms interval starting 10 ms after

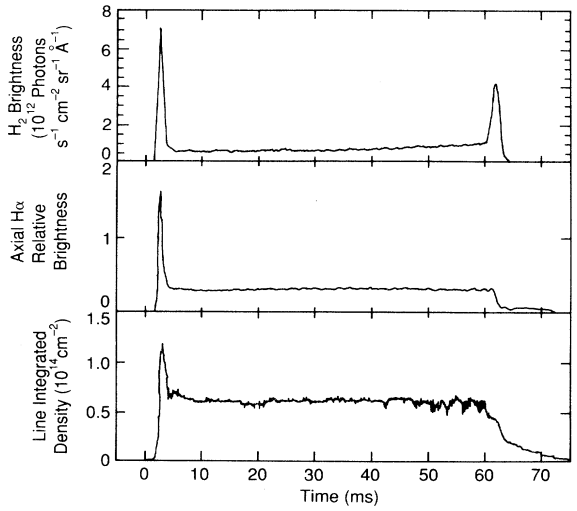

FIG. 8. Plots of the gas port 2800 Å continuum brightness, axially integrated H_α relative brightness, and line-integrated electron density versus time.

discharge initialization. The brightness has a fairly smooth wavelength dependence, consistent with a continuum, with a maximum of 7.5×10^{11} photons s^{-1} cm^{-2} sr^{-1} Å^{-1} at 2800 Å. Deviations from a smooth wavelength dependence are probably due to variations in either electron temperature or density, neither of which was measured in the gas box. Several measurements at wavelengths between 2960 and 3200 Å were omitted from the brightness plot due to contamination by impurity spectral line emission, which showed large variations in intensity during the discharge, as opposed to the nearly constant atomic and molecular hydrogen emission [3]. Also plotted in Fig. 9 is a curve of the (normalized) measured continuum spectrum for decays from the $v'=0$ vibrational level of the a state [21]. The calculated curve

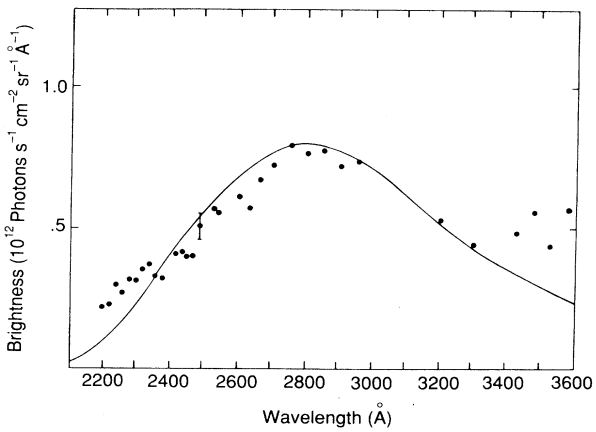

FIG. 9. Plot of the continuum brightness from 2200 to 3600 Å at the gas port. The error bar indicates the experimental uncertainty.

matches the measured curve fairly well between 2350 and 3300 Å. Both curves peak at 2800 Å, suggesting that much of the continuum emitted by the Tara plasma arose from decays from the $v'=0$ level.

In general, continuum emission from a hydrogen plasma is comprised of molecular hydrogen, bremsstrahlung (free-free), and recombination (free-bound) continua. Near-ultraviolet continuum emission from the Tara plasma was identified as being virtually all molecular in origin, due to its wavelength and axial distributions and temporal behavior. As an additional test, the expected bremsstrahlung and recombination continuum level can be calculated and compared with the measured continuum intensity. At an electron temperature of 100 eV, bremsstrahlung emission is a factor of 20 more intense than emission from recombination to the $n=2$, 3, and 4 levels, which contribute 95% of the recombination radiation in the near ultraviolet [24]. Thus we need only calculate the expected bremsstrahlung brightness level. The bremsstrahlung emissivity per unit wavelength E_B from a plasma with electron density n_e (cm^{-3}), ion density n_i (cm^{-3}), electron temperature T (eV), and effective ion charge Z_{eff} at a wavelength λ (Å) is given by

$$E_B = C g_{ff} n_e n_i Z_{\mathrm{eff}}^2 \lambda^{-1} T_e^{-1/2} e^{-hc/\lambda T_e} \quad \text{photons s}^{-1}\,\text{cm}^{-3}\,\text{sr}^{-1}\,\text{Å}^{-1}\,, \tag{3}$$

where C is 7.2×10^{-15} and g_{ff} is the free-free Gaunt factor. For an electron temperature of 100 eV, the Gaunt factor for emission at 2700 Å is 1.2±0.2. For chord-averaged Tara plasma parameters the calculated bremsstrahlung emissivity at 2700 Å is 2.2×10^{6} (±20%) photons $\mathrm{s}^{-1}\,\mathrm{cm}^{-2}\,\mathrm{sr}^{-1}\,\text{Å}^{-1}$, yielding an approximate central chord brightness of 6.6×10^{7} (±20%) photons $\mathrm{s}^{-1}\,\mathrm{cm}^{-2}\,\mathrm{sr}^{-1}\,\text{Å}^{-1}$. The measured brightness of 7×10^{11} photons $\mathrm{s}^{-1}\,\mathrm{cm}^{-2}\,\mathrm{sr}^{-1}\,\text{Å}^{-1}$ at 0 cm is a factor of 10 000 higher than the expected bremsstrahlung level, and even at 110 cm the measured brightness is a factor of 250 above the expected bremsstrahlung level, which supports the dissociative continuum as the cause of the emission.

IV. ANALYSIS

A. Rotational and vibrational temperatures

In the low density ($\sim3\times10^{11}$ cm^{-3}) Tara edge plasma, excited molecular states are populated primarily through collisions between electrons and ground state molecules. Therefore the emissivity $E_{v'}$ of a line from vibrational level v' of G is given by

$$E_{v'} = n_e \sum_v n_v \langle \sigma_v v \rangle\,, \tag{4}$$

where n_v is the density in vibrational level v of the ground state, σ_v is the emission cross section for excitation from level v of X to level v' of G and subsequent decay in the visible channel (σ_v incorporates the branching ratio), and $\langle \sigma_v v \rangle$ is the Maxwellian-averaged emission rate coefficient. The emission cross section for an arbitrary v level can be expressed as

$$\sigma_v = \sigma_R \left[\int \phi_v \phi_{v'} dr \right]^2\,, \tag{5}$$

where ϕ_v and $\phi_{v'}$ are the vibrational wave functions in the X and G states, respectively, r is the internuclear coordinate, and σ_R is the "reduced cross section," which depends on the electronic and rotational wave functions, but not on the vibrational wave functions [25]. The square of the overlap integral in Eq. (5) is known as the "Franck-Condon factor" $F(v,v')$. The emissivity can therefore be expressed as the product of the electron density, the rate coefficient, and the sum over the products of ground state vibrational level densities and corresponding Franck-Condon factors:

$$E_{v'} = n_e \langle \sigma_R v \rangle \sum_v n_v F(v,v')\,, \tag{6}$$

where $\langle \sigma_R v \rangle$ is the "reduced rate coefficient."

If rotational and vibrational levels are distributed in thermal equilibrium at 300 K, the H_2 density could be computed from a measurement of $G \rightarrow B$ line emissivity using the measured 300 K cross sections [13] and Eq. (4). Measurements of the relative intensities of individual rotational transitions within a particular vibrational band can be used to determine whether the rotational temperature is 300 K. In thermal equilibrium the rotational level distribution $f(j)$ in a particular electronic and vibrational state is given by

$$f(j) \propto (2j+1) e^{-j(j+1)U_r/kT_r}$$

where j is the rotational quantum number, U_r is the rotational quantum, k is Boltzmann's constant, and T_r is the rotational temperature. The rotational quantum of the ground state is equal to 0.003 eV, which corresponds to a temperature of 40 K. Therefore at 300 K, there will be a significant population of levels with $j>0$. Temperature variations of more than 40 K would cause significant changes in rotational level populations, and therefore in relative line intensities within vibrational bands. Comparison of the Tara (0,0) band spectrum at 0 cm shown in Fig. 3 with the 300 K (0,0) band spectrum in Fig. 4 shows that relative Tara line intensities within the (0,0) band compare closely with those in the 300 K spectrum, which are proportional to the 300 K emission cross sections. For example, the ratio of the 4634 Å line intensity to the 4628 Å line intensity is 2.0, while the ratio of their 300 K cross sections is 2.2. Examination of the (1,0) band spectrum at 4200 Å shown in Fig. 5 also shows a close correspondence between line intensity ratios and corresponding 300 K cross section ratios, with maximum ratio differences of 12%. Thus, within the uncertainties, the line spectra within the (0,0) and (0,1) bands are equivalent to those produced by H_2 at a T_r of 300 K, limiting the range of the rotational temperature to $250 < T_r < 350$ K. Note that the rotational level distribution is not necessarily thermal, and that T_r could correspond to an "average" rotational energy. Thermal rotational distributions have been measured in bucket source plasmas resulting in temperatures in the range $340 < T_r < 530$ K [26,27].

In thermal equilibrium the vibrational level distribution $g(v)$ of a particular electronic state is given by

$g(\nu) \propto e^{-U(\nu)/kT_\nu}$ where $U(\nu)$ is the vibrational energy and T_ν is the vibrational temperature. The energy of the $\nu=1$ level is 0.45 eV, which corresponds to a temperature of 5000 K. Thus, at a vibrational temperature of 300 K, virtually all of the molecules would be in the $\nu=0$ level. If the vibrational levels were in a 300 K thermal distribution the ratio of the (0,0) to (0,1) band intensities would equal the ratio of their corresponding 300 K cross sections, so we compare the intensities of the strongest lines in the two bands to determine whether the Tara H_2 spectrum is consistent with a 300 K vibrational temperature. The ratio of the (0,0) 4634 Å line to (0,1) 4205 Å line intensities is 2.1, while the ratio of their corresponding 300 K cross sections is 1.0 [15]. Thus emission from the $\nu'=0$ level of G from the Tara plasma is enhanced by a factor of 2 relative to emission from the $\nu'=1$ level, as compared with the 300 K case, indicating that a significant fraction of the molecules in Tara were in levels with $\nu>0$, and therefore that the vibrational levels were not in a 300 K thermal distribution.

The effect of a significant $\nu>0$ population on the ratio of the emissivities of the 4634 and 4205 Å lines, $E_{4634\text{ Å}}/E_{4205\text{ Å}}$, can be understood from the relationship between the emissivity, ground state vibrational level densities, and Franck-Condon factors [Eq. (6)]. Using Eq. (6), the emissivity ratio can be expressed as

$$E_{4634\text{ Å}}/E_{4205\text{ Å}}=\sum_\nu n_\nu F(\nu,0)/\sum_\nu n_\nu F(\nu,1)\ , \tag{7}$$

where $F(\nu,0)$ and $F(\nu,1)$ are the Franck-Condon factors for coupling to the 0 and 1 levels of G. If the ν dependence of the Franck-Condon factors is significantly different for these two levels, the $E_{4634\text{ Å}}/E_{4204\text{ Å}}$ ratio will depend on the ground state vibrational distribution. Since G is a Rydberg state, the shape of the potential energy curve of the G state close to the minimum can be approximated by the H_2^+ ground state curve, and therefore the Franck-Condon factors for coupling between the H_2 ground state and low ν' levels of G will be nearly equivalent to the factors for coupling between the H_2 ground state and the low ν' levels of the H_2^+ ground state. The ratio of Franck-Condon factors for coupling to the $\nu'=0$ level of G increases by a factor of 4 between the $\nu=0$ and 1 levels of X [28]. Thus a relatively small $\nu=1$ population will cause $\nu'=0$ emission to be enhanced over emission from $\nu'=1$, which could explain the factor of 2 increase in $E_{4634\text{ Å}}/E_{4205\text{ Å}}$ relative to their 300 K, cross section ratio.

It is impossible to determine the vibrational distribution from measurements of only two band intensities. However, population of levels with $\nu>0$ indicates a vibrational "temperature" significantly greater than 300 K, since the $\nu=1$ level is 0.45 eV above the $\nu=0$ level. These measurements do not constrain the upper limit of the vibrational temperature, but it is unlikely that it is greater than 3 eV (34 800 K), the upper limit of the kinetic temperature determined from linewidth measurements [3]. Vibrational distributions have been measured in bucket source plasmas and found to be nonthermal, with temperatures in the range 1300–2500 K [26,27].

The relatively high vibrational temperatures measured in the bucket source plasmas and inferred from Tara measurements are most likely due to electron collisional excitation processes. A molecule in the $\nu=0$ level of the ground state X is excited by electron collision to any vibrational level in the B,C, or D states. The molecule then decays back to any vibrational level of the X state. Molecules which decay into a level with $\nu>0$ will remain in that level until reexcited, ionized, or dissociated, leading to significant population of these levels. An upper limit for the density of H_2 in these levels due to this two-step excitation and decay mechanism can be computed using a simplified rate equation for the density of H_2 which has undergone excitation to the B,C, or D states, denoted by n^*,

$$dn^*/dt=n_e n_0 Q_e-n_e n^* Q_{i,d}\ , \tag{8}$$

where n_0 is the density of the molecules in the $\nu=0$ level of the ground state, Q_e is the rate of excitation to the B,C, or D states, and $Q_{i,d}$ is the sum of the ionization and dissociation rates. In steady state, $n^*/n_0=Q_e/Q_{i,d}$. Using the rates for excitation, ionization, and dissociation at an electron temperature of 100 eV given in Ref. [23], $n^*/n_0=0.5$, giving an upper limit of 33% for the fraction of molecules in levels with $\nu>0$. This two-step level mixing results in a rotational distribution similar to the initial 300 K thermal distribution, since $|\Delta j|<1$ for a single transition. This explains the narrow range of rotational temperatures found in the bucket source and Tara plasmas.

B. Molecular density spatial distribution

The molecular density in Tara can be determined within limits from line emissivity measurements. The emissivity of the strongest line, $E_{4634\text{ Å}}$, can be expressed as the sum of the contribution from the ground state $\nu=0$ level and levels with $\nu>0$ [from Eq. (6)]:

$$E_{4634\text{ Å}}=n_e\langle\sigma_R v\rangle n_M F(0,0) \times\left[n_0/n_M+\sum_\nu n_\nu F(\nu,0)/[n_M F(0,0)]\right]\ , \tag{9}$$

where n_0 is the density in the $\nu=0$ level, n_M is the total density, and the sum extends from $\nu=1$ to 15. From Sec. IV A, $0.66<n_0/n_M<1.0$, and from Ref. [28] $0<F(\nu>0,0)/F(0,0)<2$. Therefore the emissivity can be expressed as

$$E_{4634\text{ Å}}=1.2 n_e\langle\sigma v\rangle_{4634\text{ Å}} n_M \tag{10}$$

to within 40%, where $\langle\sigma v\rangle_{4634\text{ Å}}$ is the Maxwellian-averaged emission rate coefficient using the effective emission cross section given in Ref. [15]. Note that this emissivity is only 20% higher than that for the case in which all molecules are in the $\nu=0$ level.

The radial molecular density profile inferred from the 4295 Å emissivity profile using Eq. (10) is plotted in Fig. 10. Note that the density at radii less than 10 cm is zero, since the emissivity in this range was set to zero to avoid negative values. The radial atomic hydrogen density at

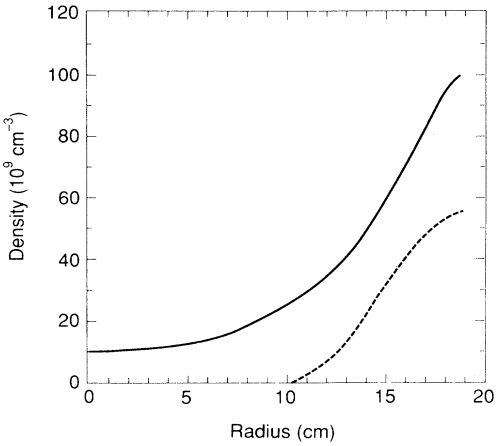

FIG. 10. Plot of the H_2 (dashed line) and H (solid line) radial density profiles at 110 cm.

100 cm inferred from H_α emissivity measurements [3] is also plotted for comparison. The H_2 is confined to an outer shell, while the atomic hydrogen penetrates to the center, attenuated by a factor of 10. The molecular density at 18 cm is 6×10^{10} cm^{-3} ($\pm40\%$), which is within a factor of 2 of the atomic density at the same radius. The FIG edge pressure interpolated at 110 cm was 2.7×10^{-6} torr, indicating a density of 10^{11} cm^{-3}.

The molecular radial density profile can be understood in terms of the mean free path l, given by $l=v/(n_eQ)$, where v is the mean particle speed and Q is the sum of all dissociation and ionization rate coefficients. The molecular kinetic temperature is expected to be equal to the rotational temperature, since any heavy particle collisions which change the rotational energy would affect the kinetic energy similarly. The mean molecular speed at 300 K is 1.6×10^5 cm s^{-1}, and the molecular ionization and dissociation rate coefficients (including continuum dissociation and dissociation into excited states) for a 100 eV electron temperature plasma are 5×10^{-8} and 8×10^{-9} cm^3 s^{-1}, respectively [23]. Using the mean electron density, 10^{12} cm^{-3}, the molecular mean free path is 2.7 cm, consistent with the hollow radial molecular density profile inferred from chordal emissivity measurements.

The axial dependence of the H_2 density may be inferred from the central chord line emissivity measurements made at 0, 30, and 110 cm plotted in Fig. 6. Since the ratios of line intensities between different vibrational and rotational levels are independent of axial position, the ground state vibrational and rotational distributions are assumed to be constant along the axis. Therefore the axial H_2 density follows the axial H_2 line intensity. A maximum density of 4×10^{12} cm^{-3} is obtained at the gas injection port. Note that both the molecular and atomic emission approximately follow the FIG pressure, with the atomic intensity drop between 0 and 30 cm more closely matching the FIG pressure drop. This suggests that the FIG's measured atomic rather than molecular edge density, which seems reasonable, since molecules leaving the wall would not reach the FIG inlet flange before being ionized or dissociated. The molecular axial scale length obtained from central chord emission measurements is 13 cm between 0 and 30 cm, and 61 cm between 30 and 110 cm. These scale lengths are large compared with the calculated molecular mean free path of 2.7 cm, indicating a source of molecules away from the gas port, such as the wall. Atoms hitting the wall can stick and recombine with other atoms to form molecules, which can be desorbed through atomic bombardment and then enter the plasma, where they are ionized or dissociated (recycling).

C. Molecular contribution to H_α emission through dissociative excitation

The H_2 line intensity measurements can be used to determine the fraction of atomic H_α emission caused by molecular dissociative processes, and thus allow the atomic hydrogen density to be obtained unambiguously from H_α emission measurements. In a hydrogen plasma there are two collisional processes which produce H_α emission: collisional excitation of atomic hydrogen and collisional dissociative excitation of molecular hydrogen. Emission through dissociative excitation is described by

$$e+H_2\rightarrow e+H_2(2p\Sigma_u^+;n=3)\rightarrow H+H(n=3)\ , \quad (11)$$

where $H_2(2p\Sigma_u^+;n=3)$ represents H_2 in the $2p\Sigma_u^+$ state, which dissociates into one ground state atom and one atom in the $n=3$ state. The H_α emissivity contribution from atomic excitation, $E_{H_\alpha,A}$, is given by $E_{H_\alpha,A}=n_An_e\langle\sigma v\rangle_{H_\alpha,A}$ where n_A is the atomic ground state density and $\langle\sigma v\rangle_{H_\alpha,A}$ is the rate coefficient for atomic emission of H_α through electron collisional excitation. The H_α emissivity contribution from molecular dissociative excitation, $E_{H_\alpha,M}$, is given by $E_{H_\alpha,M}=n_Mn_e\langle\sigma v\rangle_{H_\alpha,M}$, where $\langle\sigma v\rangle_{H_\alpha,M}$ is the rate coefficient for molecular dissociative excitation to produce H_α emission. From Eq. (10), the product of the molecular and electron densities n_Mn_e can be expressed as the ratio of the 4634 Å emissivity to the effective emission rate coefficient: $n_Mn_e=0.86E_{4634\text{ Å}}/\langle\sigma v\rangle_{4634\text{ Å}}$. Therefore the molecular fraction of the H_α emissivity can be expressed as

$$E_{H_\alpha,M}/E_{H_\alpha,t}=0.86(\langle\sigma v\rangle_{H_\alpha,M}/\langle\sigma v\rangle_{4634\text{ Å}})\times(E_{4634\text{ Å}}/E_{H_\alpha t})\ , \quad (12)$$

where $E_{H_\alpha,t}$ is the total H_α emissivity. At an electron temperature of 100 eV, the ratio of the rate coefficients is equal to 30 [25]. Thus the molecular H_α emissivity fraction is given by

$$E_{H_\alpha,M}/E_{H_\alpha,t}=27E_{4634\text{ Å}}/E_{H_\alpha,t} \quad (13)$$

($\pm40\%$). At 110 cm, and at a 16 cm radius, the ratio $E_{4634\text{ Å}}/E_{H_\alpha,\text{tot}}$ equals 1/500, yielding a molecular H_α emissivity contribution of $(5.4\pm2.2)\%$.

D. Molecular ionization rate

Molecular line spectra measurements can be used to infer the molecular ionization rate in the same way that H_α emission measurements are used to infer the atomic hydrogen ionization rate. The molecular ionization rate Γ_M is given by $\Gamma_M = n_M n_e S_M$, where S_M is the molecular ionization rate coefficient and it is assumed that nearly all molecules are in the ground electronic state. Substituting for the product of molecular and electron densities given in Sec. IV we obtain

$$\Gamma_M = 0.86 E_{4634\ \text{Å}} S_M / \langle \sigma v \rangle_{4634\ \text{Å}} .$$

The ratio of the molecular ionization rate coefficient to the 4634 Å line excitation rate coefficient at 100 eV is 5000 [23]. Therefore, the molecular ionization rate is given by $\Gamma_M = 3300 E_{4634\ \text{Å}}$ (this ignores ionization from excited electronic levels, which is negligible for the low density plasmas considered here). Similarly, ignoring the 5.4% molecular contribution, the atomic ionization rate Γ_A for electron temperatures above 10 eV and densities below 10^{13} cm^{-3} can be approximated from a measurement of the H_α emissivity: $\Gamma_A = 10 E_{H_\alpha, t}$ [29].

The molecular ionization radial profile was computed using the 4634 Å emissivity profile and is plotted in Fig. 11. Also plotted on the same graph are the atomic ionization profile obtained from the H_α emissivity measurements [3] and the sum of the atomic and molecular ionization rates. Note that the molecular ionization is nonzero only at the plasma edge, as follows from the H_2 radial emissivity profile, while the atomic ionization is approximately constant across the plasma. The concentration of plasma fueling at the edge contrasts with the electron density radial profile, which is peaked at the center [1], suggesting a lower confinement time at the plasma edge than in the center or an inward pinch.

The total molecular and atomic ionization rates $\Gamma_{i,t}$, assuming azimuthal symmetry, are given by $\Gamma_{i,t} = \int \Gamma_i 2\pi r\, dr\, dz$, where i represents atoms (A) or molecules (M) and the integral extends over the plasma volume. If it is assumed that the radial profile is constant along the axis, the total ionization rates can be computed by scaling the rate at 110 cm with local FIG and central chord H_α measurements, resulting in molecular and atomic ionization (fueling) rates of 254 and 206 A, respectively, for a total of 460 A.

The global particle confinement time τ_p may be computed from the total fueling rate $\Gamma_t = \Gamma_{M,t} + \Gamma_{A,t}$; $\tau_p = N_e / \Gamma_t$, where N_e is the total electron number. Integrating the electron density over the plasma volume yields a value of 1.5×10^{18} electrons. The total fueling rate was 2.9×10^{21} electron/s, giving a τ_p of 0.52 ms compared to the energy confinement time of 0.25–0.5 ms [1]. Note that, if molecular ionization were ignored, τ_p would increase approximately by a factor of 2.

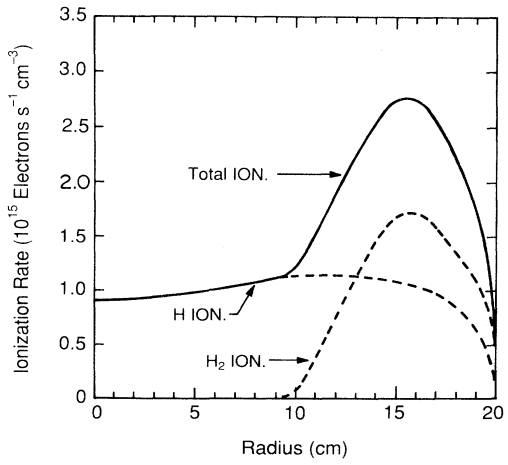

FIG. 11. Plot of the H_2, H, and total (summed) radial ionization profiles at 110 cm.

E. Molecular dissociation rate

Just as H_2 line emission measurements may be used to infer the molecular ionization rate, dissociative continuum emission measurements make it possible to obtain the $X\ ^1\Sigma_g^+ \rightarrow a\ ^3\Sigma_g^+ \rightarrow b\ ^3\Sigma_u^+$ dissociation rate. Each dissociation event is accompanied by emission of a continuum photon, so the dissociation rate follows from a measurement of wavelength-integrated continuum emissivity. The wavelength scan of the Tara spectrum at the gas port extended from 2200 to 3600 Å, and there were additional measurements at 4200 and 4640 Å, which showed emissivity levels equivalent to those at 3600 Å. For the purpose of computing the dissociation rate, the continuum level between 1600 and 2200 Å is assumed to be independent of wavelength and equal to the level at 2200 Å. Integrating the continuum emission at 0 cm between 1600 and 5000 Å yields a central chord brightness of 1.5×10^{15} photons s^{-1} cm^{-2} sr^{-1}. If the radial emissivity profiles of the continuum and line emission are assumed to be identical and independent of z, the total continuum emission can be estimated by scaling with the volume-integrated line emissivity, since the continuum and line intensities have the same axial profile. The resulting continuum emission rate is 5×10^{19} photons s^{-1}, corresponding to a total dissociation rate of 6 A, as compared with the molecular ionization rate of 254 A.

The ratio of molecular ionization to dissociation inferred from emission measurements is 40:1 (±50%). Since the cross sections for these two processes have a different energy dependence, this ratio is electron temperature dependent. The dissociation cross section peaks at 40 eV and decreases as E_v^{-2} beyond the threshold, where E_e is the electron energy, while the cross section for ionization peaks at 50 eV and decreases as E_e^{-1} beyond threshold [23]. As a result, the ratio of the dissociation to ionization rates follows a T^{-1} dependence for electron temperatures above 40 eV. An ionization to dissociation ratio of 40:1 is consistent with the Tara edge electron temperature of 100 eV. This agreement supports the use of the molecular continuum and line brightness measurements to obtain dissociation and ionization rates.

F. Power expended in molecular processes

The power expended in molecular ionization, dissociation, and radiation can be estimated from emission measurements. The mean energy required for molecular ionization, the most important breakup mechanism, is 16 eV, and for dissociation of H_2^+, into a ground state atom and a proton, 10 eV, for a total molecular ionization energy cost of 26 eV. Dissociation into an atom in the ground state and an atom in the $n=2$ state requires 15 eV, dissociation into a proton and ground state atom requires 18 eV, and dissociation into two ground state atoms (continuum dissociation) requires 10 eV. Part of the energy in all of these dissociation reactions, 4–8 eV, goes into the kinetic energy of the product particles and thus is not all lost to the plasma. Molecular radiation in the Lyman and Werner bands accompanies these dissociation and ionization processes at a rate of approximately 7 eV per event. The total power spent in molecular processes is computed by integrating the local power loss rates inferred from emissivity measurements over the plasma volume. The result is 8.4 kW into molecular processes, as compared with 5.1 kW into atomic processes (excluding charge exchange) [3]. Thus the power expended in neutral processes is a small fraction of the 300 kW of rf power injected into the plasma (4.5%).

V. CONCLUSIONS

Measurements of visible and near-ultraviolet molecular hydrogen line and continuum emission from the Tara central cell plasma have been used to determine molecular densities, ionization rates, contributions to atomic H_α emission, and power requirements, which are important for understanding plasma fueling and edge physics. The molecular radial density profile obtained from $G \rightarrow B$ band line intensities showed that the molecular density and fueling peaked radially at the plasma edge and axially at the gas injection port with a maximum density of 4×10^{12} cm^{-3} ($\pm40\%$). The total molecular fueling rate inferred was 254 ± 109 A as compared with 206 ± 25 A of atomic fueling, and the fraction of molecular dissociative H_α emission inferred was $(5.4\pm2.2)\%$.

A comparison of intensities of $G \rightarrow B$ line intensities within vibrational bands showed that the rotational temperature was nearly equal to the wall temperature of 300 K. This temperature is consistent with the radial density profile inferred from chord-averaged measurements, which showed molecules were unable to penetrate beyond a 10 cm radius, suggesting that molecules entered the plasma at the wall temperature and were ionized or dissociated by electron collision before undergoing collisions with heavy particles, such as atoms or protons, which could increase molecular rotational and kinetic energies. A comparison of line intensities from different vibrational bands showed that the vibrational level distribution was not consistent with a 300 K thermal distribution and that a significant population was in levels with $v>0$, which is probably due to level mixing through electron collisions.

Measurements of the near-ultraviolet and visible continuum from 2200 to 4640 Å (and extrapolation to 1200 Å) showed that emission levels were a factor of 250–10 000 higher than expected bremsstrahlung levels (depending on axial position), and the wavelength distribution approximately matched theoretical calculations of the distribution produced by decays from the $v'=0$ level of the a state, identifying the emission as the dissociative continuum. The total dissociation rate inferred was 6 A, as compared with 254 A of molecular ionization, consistent with the Tara edge electron temperature of 100 eV. Extending the lower wavelength limit of the continuum measurements from 2200 to 1200 Å would remove the uncertainty in determining the total emissivity and would shed light on the contributions of the levels with $v'>0$ to continuum emission.

These results underline the importance of considering molecular hydrogen processes in fueling studies. In the case of the Tara plasma, ignoring the molecular fueling contribution leads to a factor of 2 error in the total fueling rate. The degree to which these molecular processes are important will depend on the type of plasma. The edge plasma in Tara had a relatively high T_e, 100 eV, and low n_e, 10^{11} cm^{-3}. A high T_e increases the ratio of molecular to atomic ionization and a low n_e allows deeper penetration of H_2 into the plasma. Plasmas with lower edge T_e and higher n_e, such as tokamak plasmas, would have a smaller relative molecular contribution to plasma fueling, and H_α and continuum emission.

ACKNOWLEDGMENTS

I would like to thank the Tara group for providing the many low density plasmas which made this work possible, and Jim Terry, Katherine Kirby, Alex Dalgarno, and John King for their helpful comments. This research was funded by the United States Department of Energy, under Contract No. DE-AC02-78ET51013.

[1] R. Post *et al.*, Nucl. Fusion **27**, 217 (1987).
[2] S. Brau *et al.*, Nucl. Fusion **28**, 759 (1988).
[3] T. Moran Ph.D. thesis, Massachusetts Institute of Technology, 1989.
[4] G. Dimov, V. Zakaikakov, and M. Kishinevskii, Sov. J. Plasma Phys. **2**, 362 (1976).
[5] T. Fowler and B. Logan, Comments Plasma Phys. Controlled Fusion Res. **2**, 167 (1977).
[6] B. Cohen, LLNL Technical Report No. UCRL-53125, 1981 (unpublished).
[7] J. Terry, Bull. Am. Phys. Soc. **25**, 951 (1980).
[8] J. Terry, J. Vac. Sci. Technol. A **1**, 831 (1983).
[9] D. McNeil, Plasma Phys. Controlled Fusion **28**, 717 (1986).
[10] D. McNeil, Princeton Plasma Physics Laboratory Technical Report No. PPPL-2351, 1986 (unpublished).
[11] G. Dieke, J. Mol. Spectrosc. **2**, 494 (1958).
[12] R. Glover and F. Weinhold, J. Chem. Phys. **66**, 303 (1977).
[13] L. Woliewicz and K. Dressler, J. Mol. Spectrosc. **67**, 416 (1977).

[14] A. Hughes and P. Lowe, Phys. Rev. **21**, 292 (1923).
[15] R. Day, R. Anderson, and F. Sharpton, J. Chem. Phys. **71**, 3683 (1979).
[16] R. Anderson, J. Watson, and F. Sharpton, J. Opt. Soc. Am. **67**, 1641 (1977).
[17] A. Coolidge, Phys. Rev. **65**, 236 (1944).
[18] H. James and A. Coolidge, Phys. Rev. **55**, 184 (1939).
[19] T. Sharp, At. Data **2**, 119 (1971).
[20] T. Kwok, S. Guberman, A. Dalgarno, and A. Posen, Phys. Rev. A **34**, 1962 (1986).
[21] C. Lishawa, J. Feldstein, T. Stewart, and E. Mushlitz, J. Chem. Phys. **83**, 133 (1985).
[22] H. Drawin and H. Henning, Association-Euratom-CEA Technical Report No. EUR-CEA-FC-384, 1966 (unpublished).
[23] R. Janev, W. Langer, K. Evans, and D. Post, *Elementary Processes in Hydrogen-Helium Plasmas* (Springer-Verlag, Berlin, 1987).
[24] I. Hutchinson, *Principles of Plasma Diagnostics* (Cambridge University Press, New York, 1987), p. 132.
[25] G. Herzberg, *Spectra of Diatomic Molecules* (Van Nostrand Reinhold, New York, 1950), p. 200.
[26] J. Bonnie, P. Eenshuistra, and H. Hopman, in *Production and Neutralization of Negative Ions and Beams,* Proceedings of the Fourth International Symposium on the Production and Neutralization of Negative Ions and Beams, edited by J. Alessi, AIP Conf. Proc. No. 158 (AIP, New York, 1986).
[27] M. Pealat, J. Taran, M. Bacal, and F. Hillion, J. Chem. Phys. **82**, 4943 (1985).
[28] K. Kirby (private communication).
[29] K. Johnson and E. Hinnov, J. Quant. Spectrosc. Radiat. Transfer **13**, 333 (1973).